Estimation of Particulate Fines on Conveyor Belts by Use of Wavelets and Morphological Image Processing

Anthony Amankwah and Chris Aldrich

***Abstract*—Estimation of the amount of fines in images of mineral particles using standard segmentation approaches is difficult. In this paper, an approach based on multivariate image analysis is presented for estimation of the amount of fines in particles on conveyor belts. The approach is based on two-level wavelet decomposition and morphological image operations, followed by feature extraction from gray level co-occurrence matrices. These features could be used with a simple k nearest neighbour model to estimate the proportion of fines in particulate images. Experimental results with coal and iron ore particles show that the performance of the method can yield better results than those achievable with standard methods.**

***Index Terms*—Multivariate image analysis, particle size distribution, wavelets, textural feature extraction.**

I. Introduction

The size distribution of mineral particles is an important parameter for the efficient operation of process plants in the mining industry. In the coal industry, the presence of excessive fine material size can lead to clogging and channel flow of gas through the solids burden and potentially gross operational inefficiencies. Typically, particle size distributions in the mining industry are measured by using sieves, cyclones and sedimentation techniques.

These methods are usually time consuming, expensive and unsuitable for process control requiring information online. In contrast, computer vision is nonintrusive and can provide a rich source of information with regard to particle size and appearance that can be used online to make timely adjustments to the process if required [1]. Some of the commercial applications available include Split, Wipfrag [2], [3], [4], as well as Lynxx that is used in the South African mining industries.

There are four major processes in a machine vision system for analyzing rock particles. These are image capture and enhancement, segmentation, feature extraction and the application of domain information to recognize objects. The most difficult step in the measurement of rock particle sizes on conveyer belts is segmentation of the image, owing to the irregular shapes of the particles, their wide size distributions, as well as partial or complete obscurity of the particles. Although significant progress has been made in this regard, there is still significant scope for improvement.

In this investigation, the use of features extracted from images of the particles to predict particle size is considered. In this way, problems related to direct segmentation of the images can be avoided. After further processing with co-occurrence matrix operations, wavelet transforms, as well as features obtained from morphological operations are used as input to simple models to discriminate between ore and coal images with the varying particle sizes.

Manuscript received March 22, 2011.

Anthony Amankwah is with the Department of Process Engineering, University of Stellenbosch, South Africa, Private Bag X1, Matieland 7602 (E-mail:amankwah@sun.ac.za).

Chris Aldrich is with the Department of Process Engineering, University of Stellenbosch, South Africa, Private Bag X1, Matieland 7602 (Tel +27 021 808 4485, Fax: +27 021 808 2059, E-mail: ca1@sun.ac.za).

II. Wavelet Transforms

The wavelet transform is a useful tool for texture analysis. It provides information about the image's spatial and frequency features. The Fourier transform on the other hand shows only the frequency characteristics [5]. Since the correlation of identical patterns at different scales can be low, the application of multiresolution methods such wavelets is a suitable to deal with the problem of scale.

In two dimensions, a two-dimensional scaling function $\Phi(x,y)$, and three two-dimensional wavelets $\Psi^H(x,y)$, $\Psi^V(x,y)$ and $\Psi^D(x,y)$ are required. Each is the product of a one-dimensional scaling function Φ and corresponding wavelet Ψ. Excluding products that produce one-dimensional results, like $\Phi(x)\Psi(x)$, the four remaining products produce the separable scaling function $\Phi(x) = \Phi(x)\Phi(y)$ and separable directional wavelets $\Psi^H(x,y) = \Psi(x)\Phi(y)$, $\Psi^V(x,y) = \Phi(x)\Psi(y)$, $\Psi^D(x,y) = \Psi(x)\Psi(y)$. Given separable two-dimensional scaling and wavelet functions, the scaled and translated bases are as follows:

$$\Phi_{j,m,n}(x,y) = 2^{j/2}\Phi(2^j x-m, 2^j y-n) \tag{1}$$

$$\Psi^i_{j,m,n}(x,y) = 2^{j/2}\Psi^i(2^j x-m, 2^j y-n),\ i = \{H,V,D\} \tag{2}$$

where index i identifies the directional wavelets. The discrete wavelet transform of image, $f(x,y)$ of size $M \times N$, is then

$$W_\Phi(j_0,m,n) = \frac{1}{\sqrt{MN}}\sum_{x=0}^{M-1}\sum_{y=0}^{N-1} f(x,y)\Phi_{j_0,m,n}(x,y) \tag{3}$$

$$W^i_\Psi(j_0,m,n) = \frac{1}{\sqrt{MN}}\sum_{x=0}^{M-1}\sum_{y=0}^{N-1} f(x,y)\Psi^i_{j_0,m,n}(x,y) \tag{4}$$

where j_0 is an arbitrary starting scale and $i = \{H,D,V\}$. The W_Φ coefficients define an approximation of $f(x,y)$ at scale j_0. The W_Ψ coefficients add horizontal, vertical, and diagonal details for scales $j \geq j_0$. Normally, $j_0 = 0$ and $N = M = 2^j$, so that $j = 0, 1, 2, \ldots J-1$ and $m, n = 0, 1, 2, \ldots 2^{j-1}$.

The equations show that the wavelet transform is a measure of the similarity of the basis function and the image. Therefore, the wavelet coefficients refer to the closeness of the image to the wavelet at the current scale. In this work, the Debauchies wavelet was used as the basis function [6]. Fig. 1(b) shows the two-level wavelet transform of a rock particle image in Fig. 1(a).

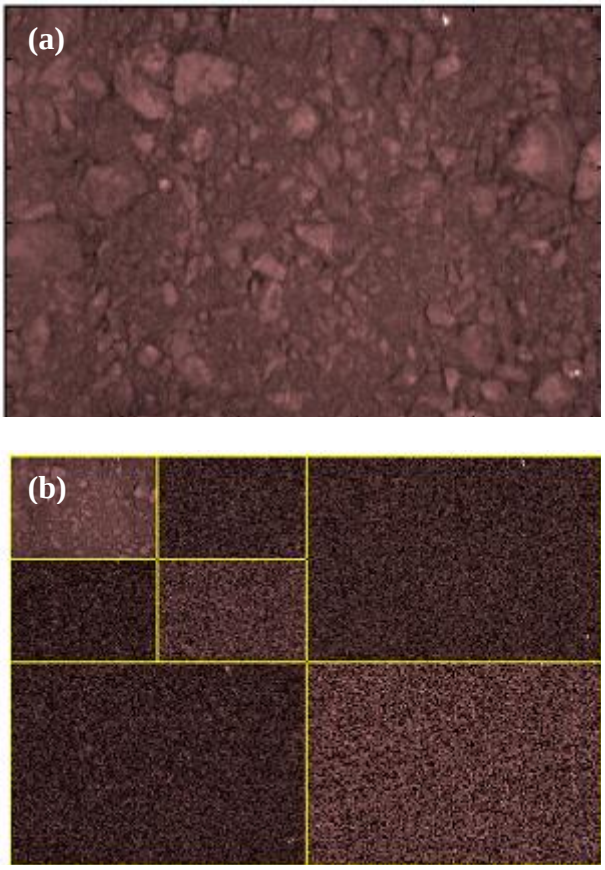

Fig.1. (a) Image of ore particles and (b) its two-level wavelet transform.

III. Morphological Operations

Mathematical morphology is the theory of the analysis of spatial structures [6],[9],[10]. It is useful for the analysis of shapes of objects of interest in images.

A. Gray-scale dilation and erosion

The gray-scale dilations and erosions are defined in terms of maxima and minima of pixel neighborhoods. It can be considered as rotating the structuring element about its origin and translating it to all locations in the image. The process is similar to convolution. Gray-scale dilation of image *f(x,y)* by structuring element SE is defined as

$$f \oplus SE = \max\{f(x-x', y-y') + SE(x', y') | (x', y' \in D_{SE})\} \quad (5)$$

where D_{SE} is the domain of *SE*, and *f(x,y)* is assumed to be equal to $-\infty$ outside the domain of *f(x,y)*. Gray-scale erosion of image f(x,y) is also defined as

$$f \oplus SE = \max\{f(x+x', y+y') - SE(x', y') | (x', y' \in D_{SE})\} \quad (6)$$

where D_{SE} is the domain of *SE*, and *f(x,y)* is assumed to be equal to $+\infty$ outside the domain of *f(x,y)*.

B. Morphological Opening

Morphological opening of an image *f(x,y)* is the erosion of *f(x,y)* followed by the dilation with the reflected structuring element *SE*.

$$f \circ SE = (f \Theta SE) \oplus SE \quad (7)$$

where Θ and $\oplus$ are erosion and dilation respectively. The structural element is must be set according to the objects of interest. Rock particles normally have oval shape. Thus, the structuring element used in this work is an ellipse.

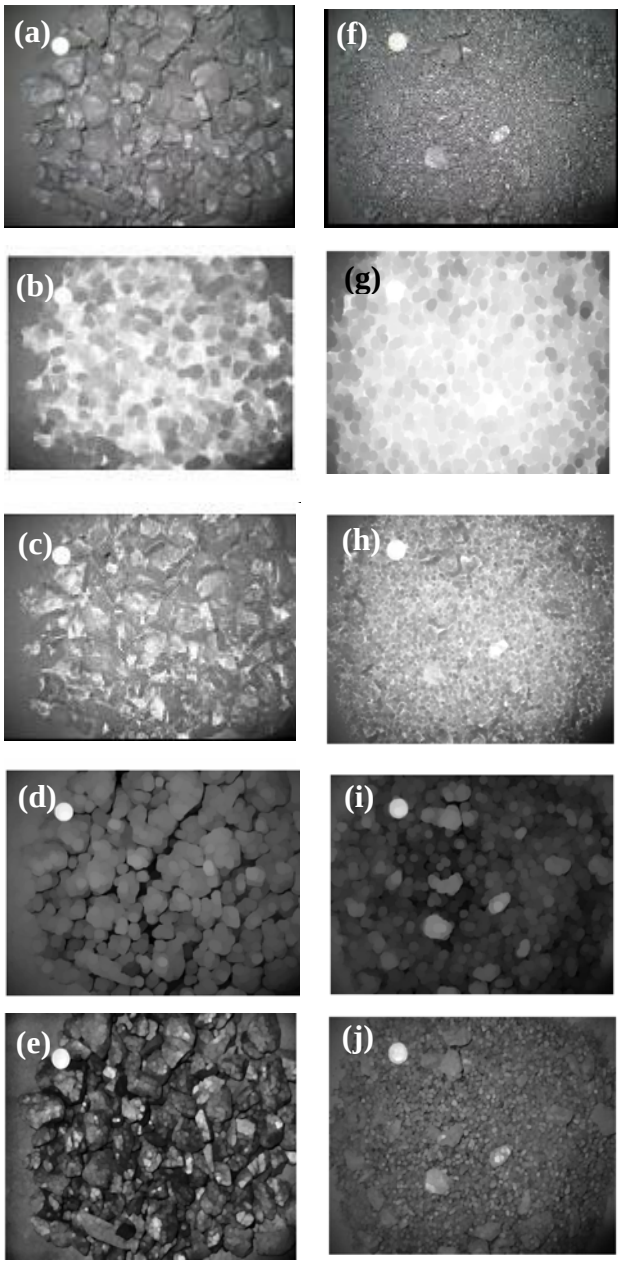

Fig. 2. (a) Rock image with 0% fines, (b) morphological closing of image in (a) with SE = 30 (c) and SE = 10, (d) morphological opening of image in (a) using a SE = 30 (e), and SE = 10 (f) Image with 80% fines (g) Morphological closing of image in (f) using SE = 30 (h), and SE = 10 (i) Morphological opening of image in (f) using SE = 30 (j) and SE =10.

C. Morphological Closing

Morphological closing is used to enhance the original

shape of the objects of interest. It is the erosion of the dilated image.

$$f \bullet B = (f \oplus SE) \Theta SE \tag{8}$$

Fig. 2 shows examples of closings and openings with structuring elements of different sizes.

IV. Feature Extraction

Feature extraction is an essential step in texture classification. Ideally, the features should contain as little redundant information as possible, without degrading the performance of the model. For this reason, feature extraction was done in two stages. The first stage consisted of extraction of wavelet coefficients and the pixel values of the morphologically filtered images. In the second stage, these features were condensed by computation of selected features from gray level co-occurrence matrices. Table 1 shows the features used to estimate the particle sizes in the images. The energy, entropy, mean and variance of the wavelet coefficients were calculated at three levels, yielding 4 x 3 = 12 features. In addition, the energy of the morphological opening coefficients with structural elements of sizes 2, 5, 10, 20 and 30, as well as the energy of the morphological closing coefficients with structural elements of sizes 2, 5, 10, 20 and 30 were calculated, yielding another 2 x 5 = 10 features.

Table 1. Features computed from gray level co-occurrence matrix f(x,y)

Feature	Equation
Energy	$\sum_x \sum_y \lvert f(x,y) \rvert^2$
Mean	$\sum_x \sum_y f(x,y)$
Entropy	$\sum_x \sum_y f(x,y) \log f(x,y)$
Variance	$\sum_x \sum_y \lvert f(x,y) - mean \rvert^2$

V. Image Classification System

In order to estimate the sizes of the particles, a k-nearest neighbor method was used, in which the amount of fines was estimated as follows:

$$SD(V) = \frac{\sum_{SD_i(V) \in N_k(V)} SD_i(V)}{k} \tag{9}$$

where $SD_i(V)$ and $N_k(V)$ are the k-closest training features and the neighborhoods respectively. The Euclidean distances of the query image and all the training set images was calculated to identify the k closest neighbors. The average of the k closest neighbors in the feature space was used as the estimate of amount of fines in the rock samples.

A block diagram of the analytical procedure is presented in Fig. 3. Co-occurrence matrices are calculated for all the images and the features mean, energy, entropy and variance are calculated for each co-occurrence matrix. The values are subsequently saved in a feature vector corresponding to each image for use with the model.

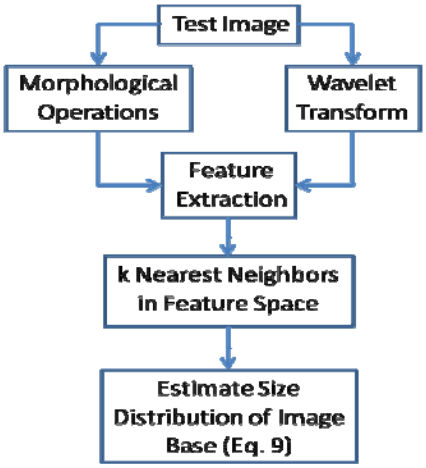

Fig. 3. Block diagram of proposed algorithm.

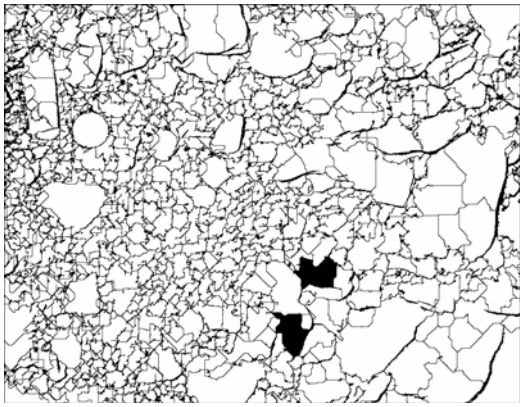

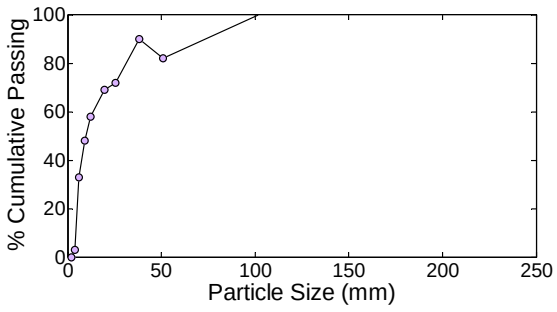

Fig. 4(a) Original image with 50% fines, (b) segmentation results from the Split software, and (c) size distribution estimation with Split software.

VI. Split Software For Size Distribution Analysis

Split image processing software is designed to estimate the size distribution of ore fragments through analyzing gray

scale images. It is the result of nine years of research at the University of Arizona in the USA. Image segmentation is one of the vital components of the Split software. Fig. 4b shows the segmentation results of original image in Fig. 4a. Note that larger particles in the images tend to be oversegmented, resulting in overestimation of the smaller particles in the image. This tends to be a general problem in image segmentation of rock particles. In principle, algorithms relying on the extraction of features from textural patterns, as well as labelled data, do not deal with this problem directly. Fig. 4c shows the plot of the size distribution estimation of the original image in Fig 4a.

VII. Experiments And Results

In order to test the efficiency and robustness proposed method two experiments were carried out. The first was based on the analysis of low grade coal and the second on the analysis of iron ore particles on conveyor belts. Instead of estimating particle size distributions consisting of a range of different size fractions, only the amount of fines in the images was considered.

A. Experiment 1

In order to compare the method outlined in the previous sections against the standard methods, coal samples were sieved on a pilot plant in to -6 mm (fine) and +6 mm (coarse) fractions. Seven different blends were created consisting of 0%, 20%, 40%, 50%, 60% 80% and 100% fines. 70 different images are processed, i.e. 10 of each grade.

Five samples of each blend were used as training data, while the rest of the images were used as test data. Fig. 5 shows typical images of the different blends. A South African five rand coin with a diameter of 25 mm is shown in each image as a measure of scale.

The 22 features that were extracted from the images with the wavelet transforms and morphological operators were highly correlated and can be visualized by considering a principal component score plot as indicated in Fig. 6. The first two principal components collectively explained almost 99% of the variance of the features. As can be seen from Fig. 6, the features associated with the seven different classes (percentage fines in the coal) could be separated well, except for the 50% and 60% fines fractions that show some overlap in the principal component score space.

Fig. 7 shows the performance of a 2-nearest neighbour classifier (triangular markers), as well as that of the Split algorithm (circular markers) against the actual proportions of fines or ground truth (broken line).

The results are further summarized in Table 2, which shows the Pearson correlation coefficients (r) between the estimated and actual values of the fines fractions for each algorithm. The correlation between D_g and D_{est} with mean values $\overline{D}_g$ and $\overline{D}_{est}$ and sample standard deviations s_g and s_{est} is defined as

$$r = \frac{E[(D_g - \overline{D}_g)(D_{est} - \overline{D}_{est})]}{s_g s_{est}} \tag{11}$$

where E is the expected value operator [11].

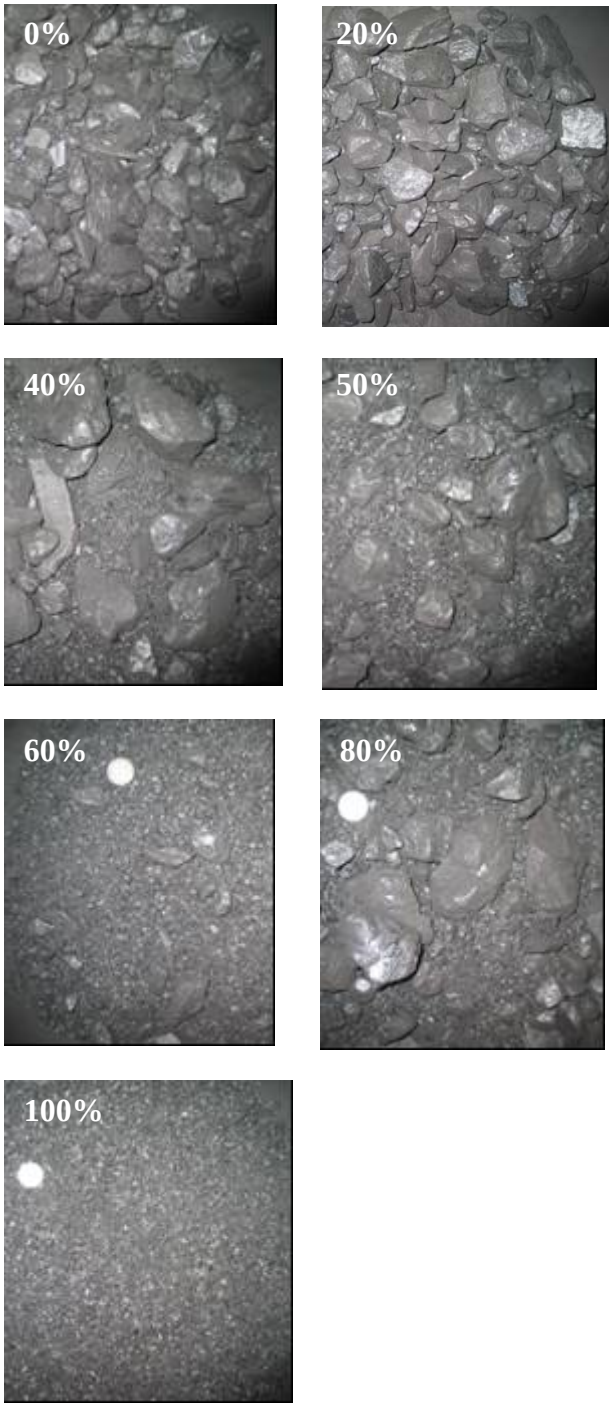

Fig. 5. Typical images of coal particle blends. Mass percentage fines are indicated on top of each image. A 25 mm diameter South African five rand coin in the bottom three images gives a sense of scale.

Table 2 also shows the average absolute difference (*AAD*) between the estimated and actual values of the fines, defined as follows:

$$AAD = \frac{\sum_{i=1}^{N} \left| D_g(i) - D_{est}(i) \right|}{N} \tag{10}$$

where N is the total number of samples and D_g and D_{est} are the ground truth and estimated size distributions respectively.

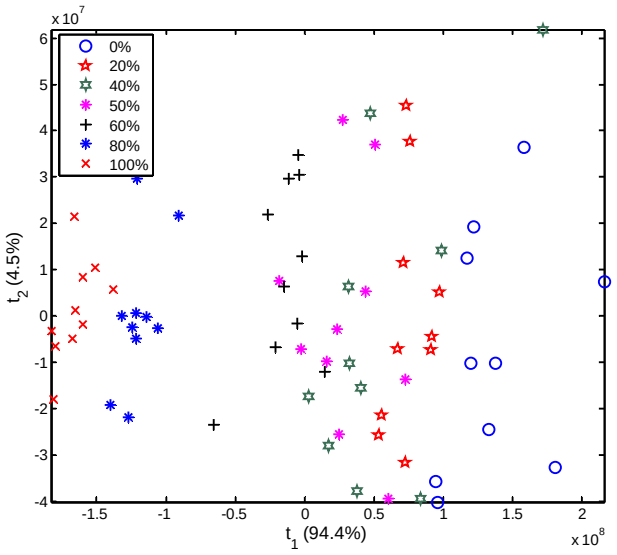

Fig. 6. Principal component scores of the 22 features extracted from the coal images in Case Study 1. The different fines fractions are indicated in the legend.

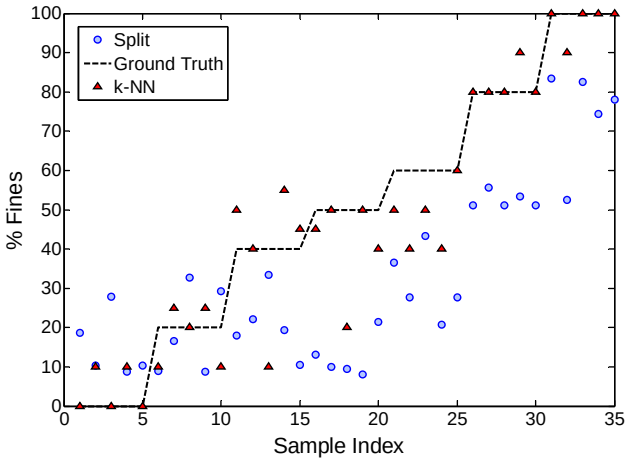

Fig. 7. Estimation of the fines in the coal samples by using Split and the k-NN classifier with the features extracted from the coal images.

TABLE 2. THE CORRELATION AVERAGE AND SUM OF ABSOLUTE DIFFERENCE BETWEEN THE ESTIMATES OF THE ALGORITHMS AND THE GROUND TRUTH FOR EXPERIMENT 1

Algorithm	Correlation (r)	Average Absolute Difference (AAD)
k-NN	0.95	6.71%
Split Software	0.81	13.8%

B. *Experiment 2*

Experiment 2 was similar to Experiment 1, except that iron ore samples were sieved on a pilot plant facility in to -6 mm (fine) and +6 mm (coarse) fractions. Five blends consisting of 0%, 10%, 20%, 30% and 100% fines were processed based on 10 images each for each blend. Fig. 8 shows typical images of the different blends.

A principal component score plot of the 22 image features is shown in Fig. 9, similar to that in Fig. 6. The first two principal components collectively explained approximately 98.5% of the variance of the features. As can be seen from Fig. 9, the features associated with the five different classes (percentage fines in the coal) could likewise be separated reasonably well, except for the 20% and 30% fines fractions that show some overlap in the principal component score space.

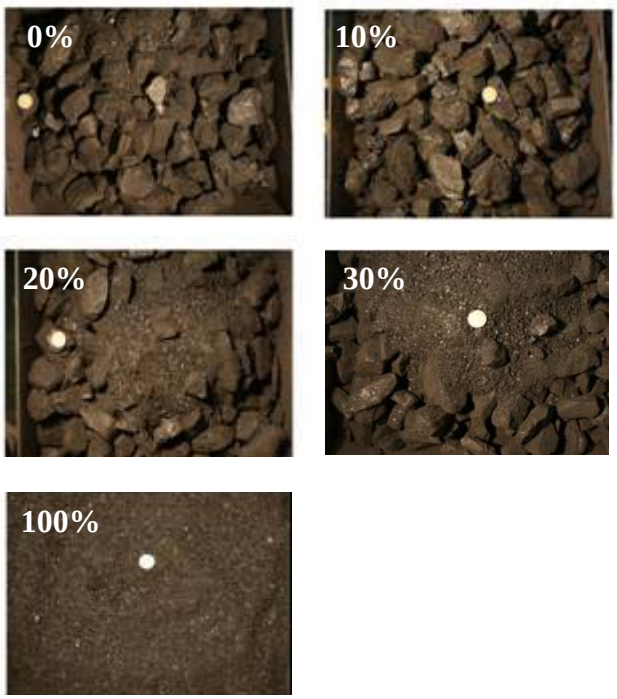

Fig. 8. Typical iron ore images showing different amounts of fines.

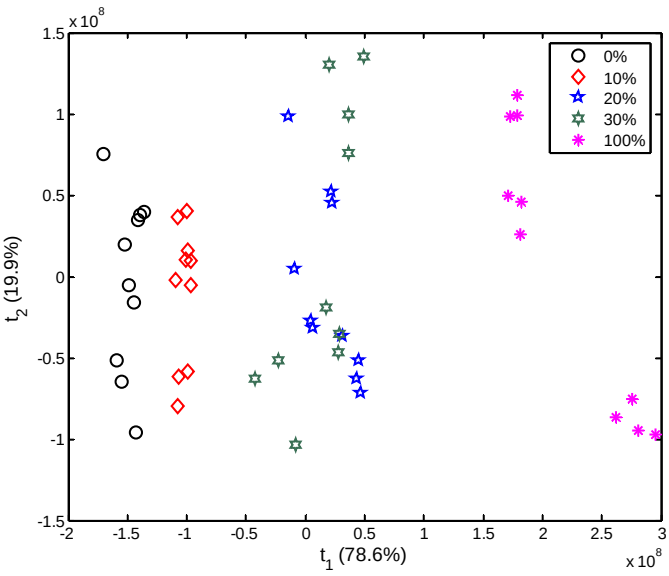

Fig. 9. Principal component scores of the 22 features extracted from the iron ore images in Case Study 2.

Fig. 10 shows the results of the estimation of fines by a 2-nearest neighbor classifier (circular markers) on 25 image samples. The estimation is compared with the ground truth (broken line). The correlation (*r*) and average absolute differences (*AAD*) between the estimates and the actual values of the fines are summarized in Table 3.

TABLE 3. THE CORRELATION AVERAGE AND SUM OF ABSOLUTE DIFFERENCE BETWEEN THE ESTIMATES OF THE ALGORITHMS AND THE GROUND TRUTH FOR EXPERIMENT 2

Algorithm	Correlation (r)	Average Absolute Difference (AAD)
k-NN	0.99	1.80%

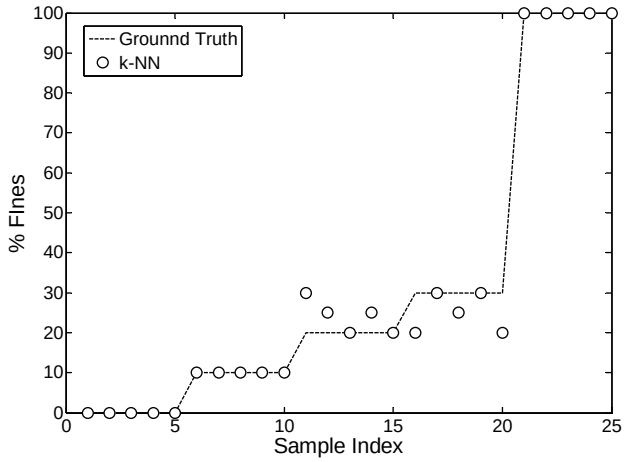

Fig. 10. Estimation of the fines in the iron ore samples by using the k-NN classifier with the features extracted from the ore images.

VIII. DISCUSSION AND CONCLUSIONS

In this paper, a method based on multivariate image analysis is proposed for estimating the amount of fines in rock and coal images. The method uses the wavelet transform and morphological operations to extract features, which are further condensed by extraction of selected features from gray level co-occurrence matrices. Further reduction of the dimensionality of the feature set could be attained with principal component analysis, but this was not explored in-depth in the present investigation.

Experimental results suggest that the performance of a simple nearest neighbour classifier can yield more reliable estimates than conventional methods. When considering fines, the range of interest in industry is from 0-30% fines, while estimates with AAD values of less than approximately 10% are considered very useful. In this respect the proposed algorithm seems especially promising.

However, unlike conventional approaches, the methodology outlined here requires exemplars consisting of labelled images, which may be difficult or costly to obtain in industrial settings. In this respect semi-supervised learning methods could also be considered.

REFERENCES

[1] G. C. Hunter, C. McDermott, N. J. Miles, and A. Singh , "A review of image analysis techniques for measuring blast fragmentation", *Mining Science and Technology*, vol. 11, no 1, July 1990, pp 19-36.
[2] J. Kemeny, A. Devgan, R. Hagaman, and X. Wu, "Analysis of rock fragmentation using digital image processing", *Geotech. Eng*., 1993, vol. 199, no.7, pp. 1144-1160.
[3] http://www.spliteng.com/ Accessed 2 March 2009.
[4] N. H. Maerz, T. C. Palangio, and J. A. Franklin , "Wipfrag image based granulometric system", *Meas. Blast Fragment*, 1996, pp. 91-99.
[5] S. G. Mallat, "A theory for multi-resolution signal decomposition: The wavelet representation". *IEEE Transactions on Pattern Analysis and Machine Intelligence.*
[6] J. Serra, *Mathematical Morphology*, vol. 1, Academic Press, London, UK, 1982.
[7] I. Daubechies, "Orthonormal bases of compactly supported wavelets", *Communications on Pure and Applied Mathematics*, 1988, vol. 41, pp. 909-996.
[8] R. M. Haralick, K. Shanmugan, and I. Dinstein, "Textural Features for Image Classification", *IEEE Transactions on Systems, Man, and Cybernetics*, 1973, Vol. SMC-3, pp. 610-621.
[9] C. R. Giardina and E. R. Dougherty, "Morphological Methods in Image and Signal Processing", Prentice-Hall, Upper Saddle River, NJ, USA, 1988.
[10] R. C. Gonzalez and R.E. Woods, "Digital Image Processing", Prentice-Hall, Upper Saddle River, NJ, USA, 2nd edition, 2002.
[11] R. G. D. Steel and J.H. Torrie, "Principles and Procedures of Statistics", New York: McGraw-Hill, 1960, pp. 187, 287.

Anthony Amankwah received a B.Sc. degree in metallurgical engineering from the Kwame Nkrumah University of Science and Technology, Kumasi, Ghana in 1996 and B.Sc. and M.Sc. degrees in electrical engineering and computer science respectively from the University of Duisburg-Essen, Duisburg, Germany in 2003. He received a Ph.D. degree in electrical and computer science from the University of Siegen, Siegen, Germany. He is currently a Postdoctoral Research Fellow at the University of Stellenbosch, Stellenbosch, South Africa. During the period 2000-2003, Dr. Amankwah held a KAAD scholarship from the Catholic Academic Exchange Service, Bonn, Germany. His research interests include machine vision, image processing, robotics, and intelligent systems.

Chris Aldrich is a Fellow of the South African Academic of Engineering and Professor and Head of the Department of Process Engineering at the University of Stellenbosch in South Africa. His research interests include machine learning, data mining and advanced process modeling and control systems in the chemical and mineral processing industries. He serves on the editorial boards of several international journals in mineral processing and process control.